ChemCatChem

Research Article
doi.org/10.1002/cctc.202400769

Chemistry Europe
European Chemical Societies Publishing

www.chemcatchem.org

Formation of a Covalent Adduct in Retaining β-Kdo Glycosyl-Transferase WbbB via Substrate-Mediated Proton Relay

Mert Sagiroglugil,[a] Qinghua Liao,[a] Antoni Planas,[b] and Carme Rovira*[a, c]

The GT99 domain of the membrane-anchored WbbB glycosyl-transferase ($WbbB_{GT99}$) catalyzes the transfer of 3-deoxy-D-manno-oct-2-acid (β-Kdo) to an O-antigen saccharide acceptor with retention of stereochemistry. It has been proposed that the enzyme follows an unprecedented double-displacement mechanism involving the formation of covalent adduct between the Kdo sugar and an active site residue (Asp232) that is properly oriented for nucleophilic attack. Here we use QM/MM metadynamics simulations on recently reported crystal structures to provide theoretical evidence for the formation of such adduct and unveil the atomic details of the chemical reaction. Our results support the interpretation made on the basis of X-ray and mass spectrometry analyses. Moreover, we show that the formation of the β-Kdo-Asp232 adduct is assisted by the sugar Kdo-carboxylate group, which mediates the transfer of a proton from Asp232 towards the phosphate leaving group, alleviating electrostatic repulsion between the two negatively charged carboxylate groups. The computed mechanism also explains why His265, previously proposed to act as a general acid, does not impair catalysis. This mechanism can be extended to other related enzymes, expanding the repertoire of GT mechanisms in Nature.

Introduction

Glycosyltransferases (GTs) constitute the main catalytic machinery for the cleavage and synthesis of glycosidic bonds in carbohydrates,[1] with great potential as biocatalysts.[2] These enzymes catalyze the formation of glycosidic linkages by the transfer of a saccharide, typically a monosaccharide, from an activated donor substrate to an acceptor substrate.[1] One of the major challenges for the rational design of specific and potent drugs/inhibitors for GTs is unravelling their detailed reaction mechanisms,[3] which are still not well understood for many GTs.

The transfer of the glycosyl group can take place either with retention or inversion of the anomeric carbon stereochemistry with respect to the donor sugar. The mechanism for inverting GTs is expected to be a typical S_N2 reaction in which the nucleophile acceptor is unprotonated by a general base,[1,4] typically a protein residue, with notable exceptions.[5] In comparison, the molecular mechanism of retaining GTs is more challenging, with two main mechanisms being currently discussed, either a double displacement reaction (by similarity to retaining glycoside hydrolases, GHs) or a front-face S_Ni type of reaction (Figure 1a,b).[6]

The double displacement reaction for retaining GTs can only be operative if there is a negatively charged residue on the beta face of the sugar that is in the proper orientation to attack the sugar anomeric carbon, a condition that few GT families fulfill (such residue has been only identified in family GT6 enzymes[6]). The current general consensus is that most retaining GTs follow a S_Ni-type of reaction in which a short-lived intermediate is formed, as early found for trehalose-6-phosphate synthase OtsA on the basis of kinetic isotope effect measurements and QM/MM metadynamics simulations,[7] and later reproduced in other retaining GTs using different levels of theory.[8] The short-lived oxocarbenium ion intermediate is stabilized by interaction with residues on the beta face of the donor sugar. Many retaining GTs display a polar side chain in this region (e.g. GalNAc–T2,[8d] LgtC[8a] and glycogenin[8e]) or a side chain carbonyl group that can stabilize the positive charge on the anomeric carbon, as in OtsA.[7b]

While the mechanism for retaining GTs with no putative nucleophile has reached a consensus among authors, the mechanism for GT6 enzymes remains to be clarified.[3a] In this case, a negatively charged residue (Glu317 in bovine α3GalT) sits on the beta face of the donor sugar, in an appropriate position to act as a nucleophile in the reaction (Figure 1b). Therefore, it is not clear whether a S_Ni-like reaction or a double-displacement mechanism can be operative. Experimental studies have shown that Glu317Ala and Glu317Gln mutants

[a] M. Sagiroglugil, Dr. Q. Liao, Prof. Dr. C. Rovira
Departament de Química Inorgànica i Orgànica (Secció de Química, (Orgànica)Institut de Química Teòrica i Computacional (IQTCUB), Universitat de Barcelona, 08028 Barcelona, Spain
E-mail: c.rovira@ub.edu

[b] Prof. Dr. A. Planas
Laboratory of Biochemistry, Institut Químic de Sarrià, Universitat Ramon Llull, Via Augusta 390
08017 Barcelona, Spain

[c] Prof. Dr. C. Rovira
Institució Catalana de Recerca i Estudis Avançats (ICREA), 08020 Barcelona, Spain

Supporting information for this article is available on the WWW under https://doi.org/10.1002/cctc.202400769

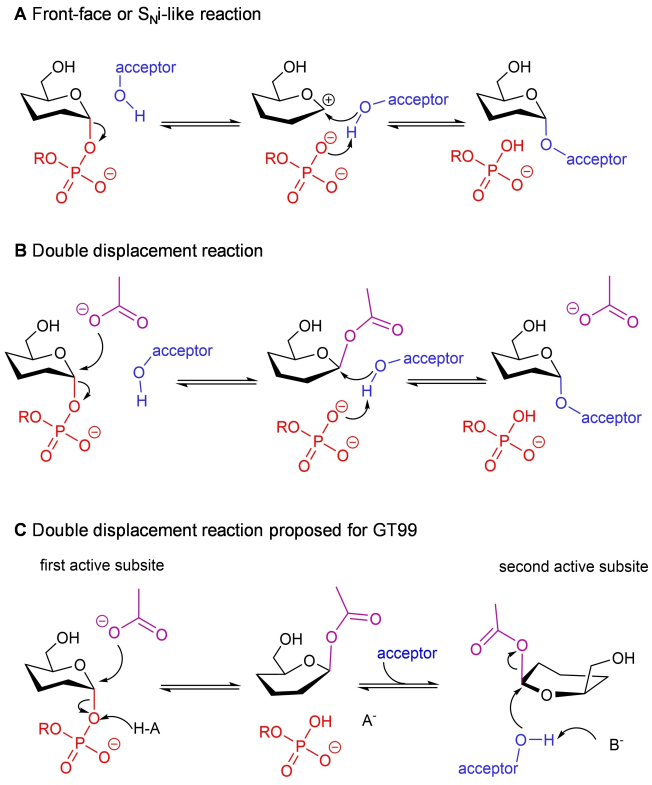

Figure 1. Proposed reaction mechanisms for retaining GTs. (A) Front-face or S_Ni-like reaction. (B) Double-displacement reaction proposed for GT6 enzymes. (C) Double-displacement reaction proposed for $WbbW_{GT99}$ based on crystal structures.

(α3GalT numbering) have none or very little activity[9], respectively, and chemical rescue experiments were successful.[9a] This is consistent with a double-displacement mechanism in which a glycosyl-enzyme covalent intermediate forms (Figure 1b). In addition, covalent adducts have been observed by mass spectrometry (MS) for human GTB, a family 6 GT that is homologous to α3GalT, upon mutation of the nucleophile to Cys.[10] The so formed sugar-Cys adduct reacts very slowly, consistent with Cys being a much poor leaving group compared to Glu. However, it is not clear whether the covalent adduct would also form in the native enzyme. Theoretical studies haven't been able to clarify it. Whereas static QM/MM calculations show that both double-displacement and S_Ni-like mechanisms are possible,[11] dynamic QM/MM simulations found that a glycosyl-enzyme intermediate is always formed.[12]

The main argument against the double displacement mechanism has been so far that the "true" GEI, *i.e.* with the native Glu (or Asp) residue, has not been observed experimentally yet. This is different from *e.g.* retaining glycosidases, in which it is enough to decrease the rate of the reaction by using fluoro-modified sugars – in combination with the use of a good leaving group such as 2,4-dinitrophenol – to trap the glycosyl-enzyme intermediate. Unfortunately, this strategy cannot be used for retaining GTs, as the leaving group (a nucleotide phosphate) cannot be replaced by another chemical group without seriously compromising binding and catalysis.

Interestingly, Forrester et al.[13] recently reported the experimental observation of a glycosyl-enzyme intermediate in a retaining GT, the family GT99 domain of WbbB from *Raoutella terrigena*. This enzyme domain transfers a β-Kdo sugar (3-deoxy-D-manno-oct-2-ulosonic acid) to an O-antigen saccharide acceptor with retention of the anomeric configuration. Kdo is an eight-carbon monosaccharide structurally related to sialic acid. Notably, the crystal structures show that the enzyme contains an Asp in the beta face of the donor sugar (Asp232) that could act as nucleophile in a double displacement reaction. Most importantly, such an adduct was identified by mass spectrometry for the first time, strongly suggesting that $WbbB_{GT99}$ follows a double displacement mechanism (Figure 1c).

There are important differences between the active sites of $WbbB_{GT99}$ and other retaining GTs so far characterized. Whereas most retaining GTs display an active site in which both donor and acceptor bind and react in the same region of the space, the $WbbB_{GT99}$ exhibits two subsites, with the sugar donor moving from one to the other during catalysis. In the first subsite (Figure 1c), the nucleophile (Asp232) can attack the anomeric carbon, forming a covalent adduct, as evidenced by MS experiments. Consistently, the structure of the Asp232Asn mutant shows that the corresponding Asp would be placed on the appropriate position to attack the sugar donor anomeric carbon. To complete the reaction, an active site histidine (His265) is proposed to assist the departure of the phosphate leaving group by proton transfer, playing the role of a catalytic acid (AH in Figure 1c). However, the His265Ala enzyme mutant retains 10% of the enzyme activity,[14] which is not fully compatible with its proposed catalytic role.

The previous structural work by Forrester et al. also reported the structure of a covalent adduct between the sugar donor and residue 232 (upon mutation of this residue to Cys or Asn, under specific conditions).[13] In these structures, the sugar donor occupies a significantly different position with respect to its position in the Michaelis complex (enzyme complex with CMP-Kdo). This was interpreted as a translocation of the donor towards another active site subsite. In the new subsite, there is a basic residue (B^- in Figure 1c, identified as Glu158 in the structures) that can deprotonate the acceptor during the subsequent glycosyl transfer step. In view of these results, a mechanism via the formation of a GEI between Kdo and Asp232 was proposed for $WbbB_{GT99}$. This mechanism is unprecedented in GTs and awaits theoretical confirmation. Therefore, here we use QM/MM metadynamics simulations to investigate the unique aspect of the proposed mechanism, which is formation of a covalent β-Kdo-Asp adduct.

Results and Discussion

Michaelis Complex Model

A structure of the complex between the WT enzyme and the CMP-β-Kdo donor is not available. However, Forrester et al.

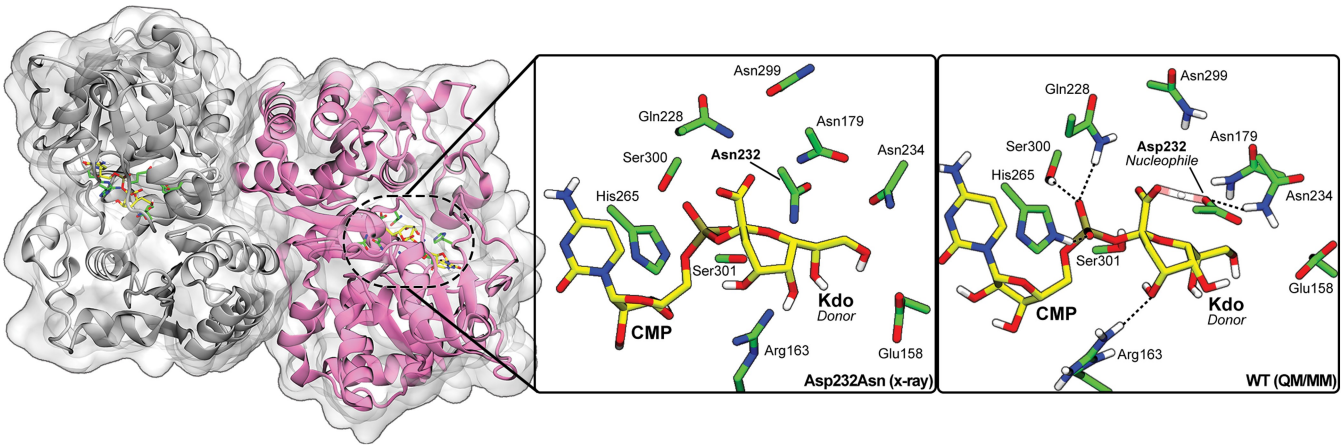

Figure 2. (A) X-ray structure of the Asp179Asn mutant of $WbbB_{GT99}$ in complex with β-Kdo-CMP (PDB 8CSB). The closest residues to the β-Kdo-CMP donor are shown. (B) Active site X-ray structure of $WbbB_{GT99}$ in complex with β-Kdo-CMP. (C) Active site structure (the mutation has been reverted) obtained from QM/MM MD simulations. Hydrogen atoms attached to C atoms have been omitted for clarity.

obtained a plausible mimic of such binary complex by mutating Asp232 to an Asn residue (Figure 2).[15] Therefore, we used this structure (PDB ID: 8CSB) to reconstruct the binary complex by reverting the mutation to the original Asp residue. Initially, we assumed that Asp232 is unprotonated (to be able to perform the nucleophilic attack) and His265 is positively charged, consistent with its proposed acidic role (Figures 1C and S1). However, in this configuration there are two carboxylates very close to each other (that of Asp232 and the carboxylate of the β-Kdo substrate, O··O = 3.4 Å), which are likely to cause strong repulsion between the two negative charges. In fact, classical MD simulations showed that this active site configuration is not stable and results in Asp232 either moving away from the active site or adopting an unreactive conformation (Figures S1 and S6), precluding the nucleophilic attack. This indicates that Asp232 is probably protonated in the enzyme-substrate complex.

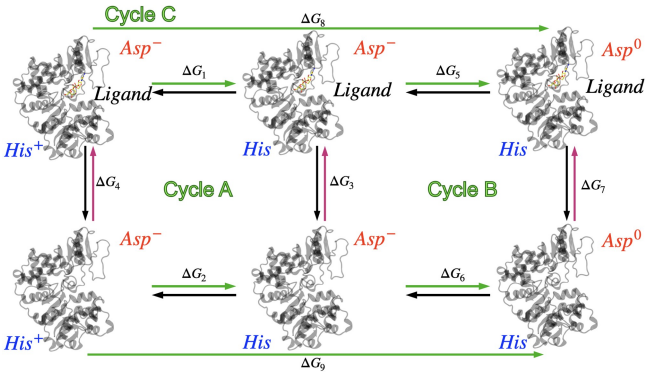

Figure 3. Thermodynamic cycles (A, B and C) that are used to calculate the relative binding free energy ($\Delta\Delta G_{bind}$) of the CMP-β-Kdo ligand in $WbbB_{GT99}$, considering different protonation states of Asp232 (negatively charged, Asp^-, or neutral, denoted as Asp^0) and His265 (positively charged, His^+, or neutral, His). Accordingly, $\Delta\Delta G_A = \Delta G_3 - \Delta G_4 = \Delta G_1 - \Delta G_2$; $\Delta\Delta G_B = \Delta G_7 - \Delta G_3 = \Delta G_5 - \Delta G_6$; $\Delta\Delta G_C = \Delta G_7 - \Delta G_4 = \Delta G_8 - \Delta G_9$.

Protonation States of Relevant Active Site Residues

To gain further insight into the protonation state of Asp232 and His265, we determined their relative pKa values in the presence or absence of the CMP-β-Kdo donor substrate, using H++ web server. Furthermore, we computed the relative binding free energies ($\Delta\Delta G_{bind}$) of the donor, using thermodynamic integration (TI) (see Methods). A thermodynamic cycle in which these two residues change protonation state in a sequential way was considered (Figure 3).

The pKa calculations show that the pKa of His265 increases from 4.1 to 6.0 upon binding of the CMP-β-Kdo donor (Figure S2), thus increasing the population of positively charged His265 from 0% to 21% at pH 7.0. This is also evident in the donor $\Delta\Delta G_{bind}$ value, computed from TI (Table S1). There is no significant change upon donor binding (-1.8 ± 1.3 kcal/mol).

In contrast, the pKa of Asp232 was found to increase significantly in the presence of the CMP-β-Kdo donor (its pKa raises from <4.0 to 7.6, Figure S2). These values indicate that, in the presentce of the donor substrate, Asp232 is mostly protonated at pH 7.0. Consistently, the TI calculations show that the relative binding free energy of the donor is -6.3 ± 2.8 kcal/mol (considering cycle B in Figure 3) or -13.0 ± 2.1 kcal/mol (considering cycle C). Therefore, it can be reasonably concluded that the neutral pair (Asp^0/His in Figure 3) is the preferred configuration of $WbbB_{GT99}$ in complex with the CMP-β-Kdo donor. Classical MD simulations (5.9 μs) with this configuration showed that Asp232 remains close to the donor sugar, with the protonated carboxylic acid oxygen at a 4.3 Å from the anomeric carbon of the donor sugar, while forming a hydrogen bond with the β-Kdo carboxylate. This is a plausible configuration for nucleophilic attack. The position of Asp232 is also compatible with that of Asn232 in the X-ray structure (Figure 2).

QM/MM Simulations of the Chemical Reaction

A snapshot of the classical MD simulation was selected for modeling the chemical reaction, using QM/MM metadynamics. Initial QM/MM MD simulations showed that the Asp232 proton often jumps towards the Kdo carboxylate group (see Figure 2, right panel), thus it can be considered as forming a low barrier hydrogen bond (O^-_{Asp232}··H··O^-_{Kdo}, with internuclear distances of 1.2-1.3 Å in average). In this scenario, it is reasonable to think that the proton would transfer to the sugar carboxylate during the reaction, allowing Asp232 to attack the C2 atom of the Kdo sugar. QM/MM metadynamics simulations were subsequently designed to model such nucleophilic attack, using one collective variable (CV) that includes the main bonds that need to be broken or formed during the reaction, *i.e.* formation of a glycosyl-enzyme species (CV = d[C2-O_{Asp232}] − d[C2-O_{CMP}]). During the simulation, Asp232 was able to attack the anomeric carbon and form a covalent bond with it and, at the same time, transfer the carboxylate proton to the leaving group phosphate, via the β-Kdo carboxylate group. A subsequent simulation using two CVs, including proton relay from Asp (see Methods), confirmed this mechanism. The computed energy barrier (9.0 kcal/mol) to form the GEI is indicative of a feasible reaction. The results also suggests that the first step of the glycosyl transfer reaction (Figure 1C) is not rate-limiting.

Representative structures along the reaction progress (Figure 4C) show that the reaction starts with a gradual approach of Asp232 to the sugar's anomeric carbon, At the same time, the proton transfers to the C2 carboxylate group (**1** in Figure 4), which simultaneously rotates and starts pointing towards the phosphate group of CMP. Subsequently, the proton transfers to the phosphate group and the sugar-phosphate bond breaks, leading to the formation of an oxocarbenium ion-like species (**TS** in Figure 4), as evidenced by the planar conformation of the β-Kdo ring around the anomeric carbon (^4E conformation). At the **TS**, the distance between the C2 atom and its closest O atom of Asp232 amounts to ≈3.8 Å, whereas that between the phosphate and the Kdo sugar is shorter (C2-O_{CMP} ≈2.2 Å),

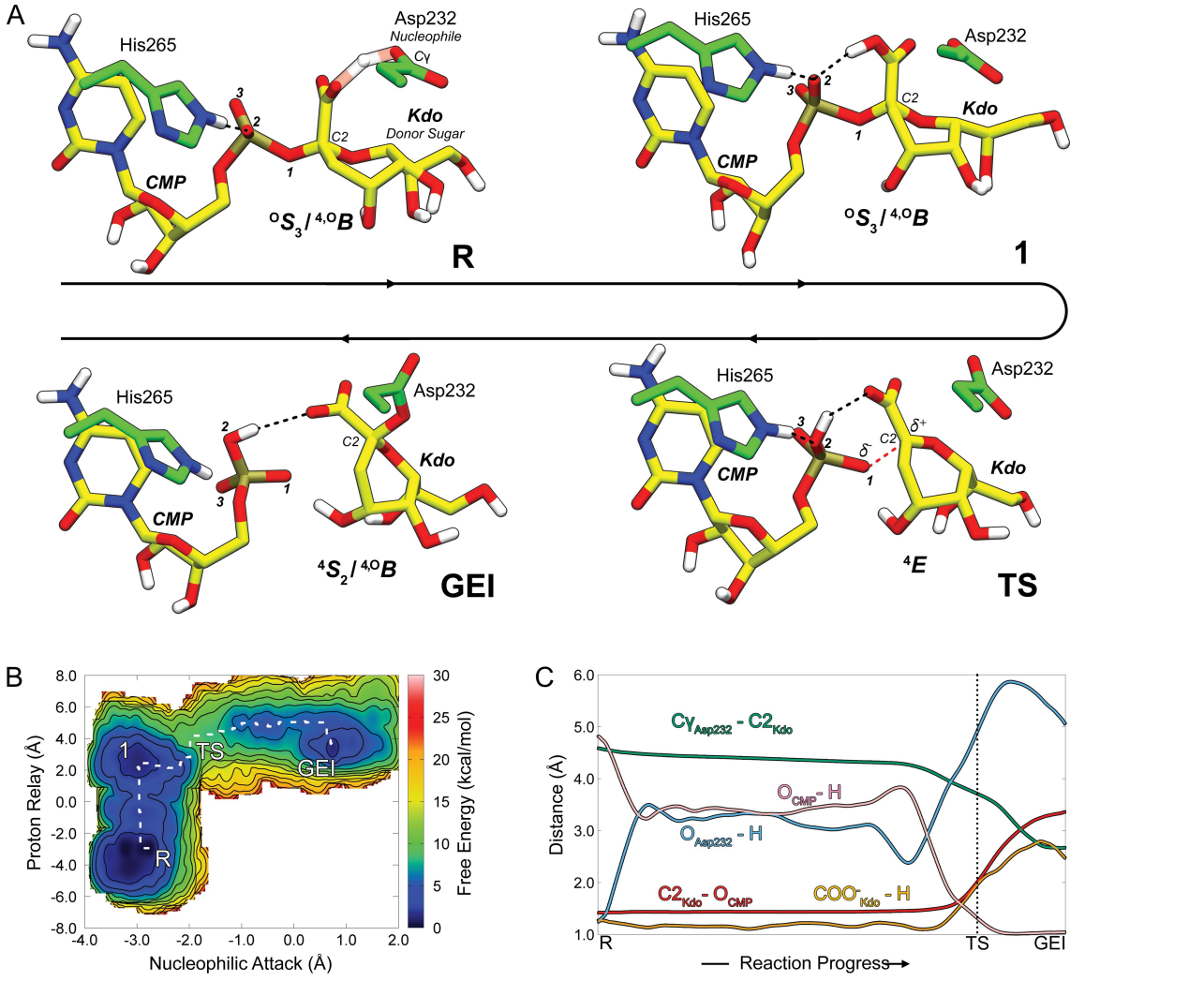

Figure 4. Formation of a covalent adduct between β-Kdo donor sugar and Asp232 in the active site of $WbbB_{GT99}$. The conformation of the kdo sugar ring is indicated. (A) Representative structures of selected states along the reaction coordinate. Hydrogen atoms attached to C atoms have been omitted for clarity. The main bond being broken at the TS is denoted with a red dashed line, whereas black dashed lines represent hydrogen bond interactions. (B) Free energy landscape of the reaction. (B) Evolution of the main catalytic distances along the reaction coordinate.

indicating a dissociative mechanism (*i.e.* the sugar-phosphate bond is being broken when Asp232 is not yet starting to form). After the **TS**, the Kdo ring changes conformation, allowing complete formation of the covalent bond between Asp232 and Kdo at **GEI**. The active site histidine, His265, forms a hydrogen bond with the CMP phosphate along the entire reaction, possibly contributing to stabilize the negative charge. Therefore, the simulations show that the Asp232 proton "travels" towards the phosphate leaving group during the reaction, thus the phosphate itself can be considered as the ultimate base of the first catalytic step.

In summary, the QM/MM metadynamics simulations provide evidence for the formation of a covalent adduct between the donor sugar and Asp232 in $WbbB_{GT99}$. The reaction is assisted by the β-Kdo carboxylate group, which mediates the transfer of a proton from Asp232 towards the phosphate leaving group. This is a clever solution that the enzyme adopts to avoid repulsive interaction between the two carboxylate groups (Kdo and Asp232), which would preclude the nucleophilic attack. This reaction has some reminiscence with the hydrolysis of carbohydrates containing neuraminic acid, which also have a carboxylate group at C2. In retaining neuraminidases, the nucleophile is a neutral Tyr that, upon deprotonation by a general base, can approach the anomeric carbon minimizing electrostatic repulsion from the sugar carboxylate. In $WbbB_{GT99}$, the nucleophile is an aspartic acid, and it does not have a basic residue close-by that can deprotonate it. In this case, electrostatic repulsion is alleviated by proton transfer to the sugar carboxylate, which can easily transfer this proton to the phosphate leaving group (Figure 5). Our mechanism also explains why His265, previously proposed to act as a general acid, does not impair catalysis.

Conclusions

In this work, we have used QM/MM metadynamics simulations to investigate the recently proposed mechanism of glycosyl-transfer in the retaining GT99 domain of the WbbB enzyme. Using the X-ray structure of the Asp232Asn enzyme mutant in complex with the β-Kdo-CMP donor, we reconstructed the binary complex of the WT enzyme and modelled the chemical reaction of GEI formation considering several protonation states of active site residues. Our results show that Asp232 should be in the protonated form to enable catalysis and that nucleophilic attack is concomitant with proton transfer from As232 to the leaving group phosphate, with the sugar carboxylate group mediating such proton transfer. This confirms the experimental proposal of the formation of a β-Kdo adduct. However, our results do not support the presence of a general acid to protonate the leaving group, rather leaving group departure is assisted by proton relay via the β-Kdo carboxylate. This mechanism, which has reminiscences with that of retaining neuraminidases, is expected to be extended to other GTs with similar architecture such as KpsC, for which a similar mechanism has been experimentally proposed very recently.[15] The results will also expand the repertoire of GT mechanisms and will aid in the development of specific inhibitors for bacterial GTs.

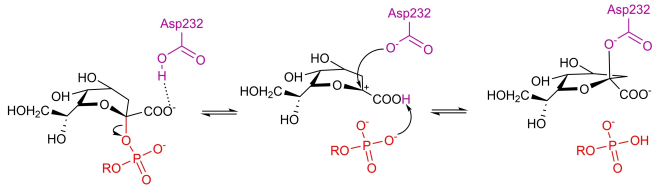

Figure 5. Schematic mechanism for the formation of a covalent β-Kdo-Asp in $WbbW_{GT99}$ proposed in this work on the basis of QM/MM metadynamics simulations.

Methods

System Preparation

An X-ray structure of WbbB GT99 from *Raoultella terrigena* (PDB ID: 8CSB)[13] was taken as the initial structure. The Asp232Asn mutation was reverted, and the crystal waters were retained. The enzyme monomer was protonated at a neutral pH with an internal dielectric of 7 using H++ server.[16] The system was enclosed in a cubic water box spanning 10 Å away from the protein surface. The net charge was neutralized by adding 21 sodium ions. RESP charges of the CMP-β-Kdo donor complex were calculated using Gaussian16 at the HF/6-31G* level of theory.

Classical MD Simulations

Classical MD simulations were carried out using the GROMACS 2022.x/2023.x software,[17] along with forcefields FF14SB,[18] GLYCAM06[19] and TIP3P[20] for the enzyme, substrate and water molecules, respectively. Input files were generated using AmberTools[21] but subsequently converted into GROMACS compatible format using the acpype software.[22] Non-bonded interactions were computed using the Verlet scheme with a neighbor search every 100 steps, and short-range electrostatic and Van der Waals cutoffs set to 10.0 Å. Particle Mesh Ewald (PME) was employed for long-range electrostatics using cubic interpolation and a Fourier grid spacing of 16 Å, along with long-range dispersion corrections for both energy and pressure. Time step was set to 2 fs for the production run. The structure was minimized using Steepest Descent and equilibrated in several steps under NVT and NPT conditions. During NVT equilibration, the system was heated to 310 K using the V-Rescale thermostat[23] for 2 ns. During NPT equilibration, the system density was regulated for 2 ns using the V-Rescale thermostat and the Parrinello-Rahman barostat.[24]

Several classical MD simulations were performed (Table S2), with a cumulative time of 8.9 μs. Each simulation used different conditions, such as varying protonation states of Asp232 and His265, as well as initial restraints to keep the position of the main active site residues and the sugar conformation (this was necessary given the limitations of classical force-fields to describe sugar ring distortions[6]). As a control, three sets of

simulations without any restraints, with different protonation states were initially run in three independent replicas, each for 500 ns. The most suitable protonation state was selected based on the analysis of the active site conformation, pKa calculations, and $\Delta\Delta G_{bind}$-TI calculations. Afterwards, other three sets of MD simulations with varying restraints in the active site were conducted to determine which structural parameters are important to match the active site configuration of the crystal structure. The most compatible state was selected and restarted for further MD sampling with gradually decreasing restraints. The trajectory was branched twice every 100 ns, resulting in 4 replicas. Each one was extended for 300 ns, 1000 ns, 1000 ns, and 300 ns, respectively. All MD simulations are summarized in Table S2 and additional information is provided in the Zenodo repository (DOI:10.5281/zenodo.11447092). One snapshot from the replica that retained a catalytically active orientation of residues, and the distortion of the sugar ring was selected as the starting point for QM/MM MD simulations.

Thermodynamic Integration and Relative Binding Free Energy Calculations

Relative binding free energy ($\Delta\Delta G_{bind}$) calculations were computed by thermodynamic integration (TI). Three sets of molecular structures with different protonation states were prepared using AmberTools.[21] For each set, the residues that were considered to change during a particular transformation cycle were excluded from the topology merging process. Additionally, three other structures without the ligand in the binding cavity were also prepared. Each transformation path consists of three steps: removing the charge of the first endpoint, transforming the VdW parameters from the first endpoint to the second endpoint and adding the charge to the second endpoint. Atomic charges were shifted linearly during charge removal and addition. Soft-core potentials were used to handle the Van der Waals transformations. Calculations were performed using pmemd.cuda of Amber 2024,[25] spanning 23 lambda windows (lambdas are evenly distributed from 0.00 to 1.00 with an increment of 0.05, and two extra lambdas 0.01 and 0.99 are added) (Figure S3) with each window running for 10 ns. The force fields used were FF14SB for proteins, GLYCAM06 for carbohydrates and TIP3P for water. Each transformation cycle was replicated three times, leading to a total simulation time of 12.42 μs. Consequently, free energy of each of the specific transition processes (ΔG_1, ΔG_2, ΔG_5, ΔG_6, ΔG_8 and ΔG_9) was calculated by integrating the average value of the potential energy change with respect to the coupling lambda over each window. Velues of $\Delta\Delta G_{bind}$ were subsequently computed according to the thermodynamic cycles of Figure 3.

QM/MM MD Simulations

QM/MM simulations were performed using the CP2 K v9.1 software.[26] One snapshot from the unrestrained classical MD simulations was used as the initial structure. The QM region includes the β-Kdo and phosphate group of the β-Kdo-CMP donor, Asp232 and His265. QM-MM boundaries include the C1-C2 bond of CMP-β-Kdo and the CA-CB bonds of Asp232 and His265. The residual QM charge was redistributed over the MM atoms of the linked residues to retain a neutral charge in the MM region. The LJ parameters of H atoms were taken from the force-field GAFF2.[27] The QM region was described by Density Functional Theory (DFT), using the Perdew-Burke-Ernzerhof (PBE) functional[28] along with molecular optimized Goedecker-Teter-Hutter (MOLOPT-GTH) pseudopotentials.[29] A triple-ζ valence polarized basis set functions (TZV2P)[30] were used to expand the Kohn-Sham orbitals, with a 350 Ry cut-off. The conjugate gradients method was used to optimize the structure, which was equilibrated under NVT conditions at 310 K maintained by a thermostat using v-rescale algorithm with a time constant of 10 fs, starting with only the substrate in the QM region (25 ps) and subsequently including protein residues Asp232 and His265 (96 ps) with an 0.5 fs time step.

QM/MM Metadynamics Simulations

The reaction mechanism was modelled with QM/MM metadynamics[31] via one collective variable, defined as the distance difference between two main chemical bonds that are formed and broken: the distance between one O atom of the carboxylic acid group of Asp232 and the anomeric carbon (O–C2) and the distance between C2 and the oxygen atom of the phosphate leaving group (C2-O_P). CP2 K, together with the Plumed 2.8 plug-in,[32] was used to run the metadynamics. An initial simulation was launched with gaussian height of 2.0 kcal·mol^{-1}, the gaussian width of 0.20 Å, and a deposition pace of 100 MD steps, corresponding to 50 fs. The simulation showed that the Asp232 binds to the anomeric carbon while the phosphate group departs from it. Simultaneously, the carboxylic acid proton of Asp232 jumps towards the β-Kdo carboxylate and later transfers to the phosphate leaving group. Unfortunately, recrossing over the TS was not possible because the phosphate proton did not return to the carboxylate of Asp232, thus the energetics of the reaction could not be quantitatively assessed. To solve this, the reaction mechanism was divided in two parts and two metadynamics simulations were subsequently performed. The first simulation (I) was aimed to describe nucleophilic attack and leaving group departure, together with the transfer of the proton from Asp232 to the sugar carboxylate. A well-tempered metadynamics using one CV (distance difference) with the following parameters was set: a Gaussian height of 2.0 kcal·mol^{-1}, the Gaussian width of 0.20 Å, a deposition pace of 100 MD steps, and a bias factor of 30. The second metadynamics simulation (II) was aimed to describe the transfer of the proton from the sugar carboxylic acid to the phosphate group of CMP. The corresponding well-tempered metadynamics used one CV (distance difference) with the following parameters: a gaussian height of 0.6 kcal·mol^{-1}, a gaussian width of 0.05 Å, a deposition pace of 100 MD steps and a bias factor of 10. This simulation was started from **GEI**, obtained after QM/MM MD equilibration (15 ps) of state **2**. Both

metadynamics (I and II) successfully achieved recrossing towards the initial configuration. A total number of 190 and 133 gaussians, respectively, were deposited. The two free energy profiles resulting from the integration of negative biases are represented in Figure S8. A snapshot corresponding to state **2** spontaneously transitions into the reaction products (the β-Kdo-Asp232 adduct), confirming that there is no significant barrier between these two states.

Another metadynamics simulation was conducted to describe the reaction in a 2D collective variable (CV) space. The first CV was chosen to represent the distance difference of the glycosidic linkage ($C2_{KDO}$ – $O1_{CMP}$) and the nucleophilic distance (O_{Asp232} – $C2_{KDO}$). The other CV represents the difference in the transferring proton distances at both ends (O_{Asp232}-H - $O2_{CMP}$-H). The well-tempered metadynamics used two CVs with the following parameters: a gaussian height of 2.0 kcal·mol^{-1}, a gaussian width of 0.20 Å and 0.10 Å, a deposition pace of 100 MD steps and a bias factor of 30. This simulation was started from **R** and successfully achieved recrossing over the **TS**. A total number of 1765 gaussians were deposited.

The free energy landscape (Figure 4b) was obtained from a reweighting process with all biases subtracted from the integration of negative biases (Figure S9). The nucleophilic attack CV is defined as the distance difference between $C2_{KDO}$ – $O1_{CMP}$ and CG_{Asp232} – $C2_{KDO}$ in the reweighted landscape. An average estimation from Scott's[33] and Silverman's[34] rules was used to set the kernel bandwidth during the reweighting process.

Supporting Information

Supporting Figures (S1-S9) and Tables (S1-S3).

Acknowledgements

We acknowledge funding from the European Research Council (ERC-2020-SyG-951231 "Carbocentre"), the Spanish Ministry of Science, Innovation and Universities (MICINN/AEI/FEDER, UE, PID2020-118893GB-100 to C. R. and PID2022-138252OB–I00 to A. P), the Spanish Structures of Excellence María de Maeztu (CEX2021-001202-M) and the Agency for Management of University and Research Grants of Catalonia (AGAUR, 2021-SGR-00680). We thank Profs. Matthew S. Kimber and Chris Withfield (University of Ghelph, Canada) for a critical reading of the manuscript and Dr. Mariana A. B. Morais (CNPEM, Brasil) for technical assistance. We are grateful for the technical assistance provided by the support of the MareNostrum IV and CTE-Power supercomputers of the Barcelona Supercomputing Center (BSC-CNS), within the Red Española de Supercomputación (RES).

Conflict of Interests

The authors declare no conflict of interest.

Data Availability Statement

The data that support the findings of this study are openly available in the Zenodo repository (https://doi.org/10.5281/zenodo.11447092), reference number [35].

Keywords: 3-deoxy-D-manno-oct-2-acid · carbohydrate-active enzymes · metadynamics · molecular dynamics •Quantum mechanics/molecular mechanics · Catalytic mechanism

[1] L. L. Lairson, B. Henrissat, G. J. Davies and S. G. Withers, *Annu. Rev. Biochem.* **2008**, *77*, 521–555.
[2] a) B. Nidetzky, A. Gutmann and C. Zhong, *ACS Catal.* **2018**, *8*, 6283–6300; b) M. M. Palcic, *Curr. Opin. Chem. Biol.* **2011**, *15*, 226–233.
[3] a) A. Ardevol, J. Iglesias-Fernandez, V. Rojas-Cervellera and C. Rovira, *Biochem. Soc. Trans.* **2016**, *44*, 51–60; b) J. Li, G. Qu, N. Shang, P. Chen, Y. Men, W. Liu, Z. Mei, Y. Sun and Z. Sun, *Green Synthesis and Catalysis* **2021**, *2*, 45–53; c) K. W. Moremen and R. S. Haltiwanger, *Nat. Chem. Biol.* **2019**, *15*, 853–864.
[4] J. F. Darby, A. K. Gilio, B. Piniello, C. Roth, E. Blagova, R. E. Hubbard, C. Rovira, G. J. Davies and L. Wu, *ACS Catal.* **2020**, *10*, 8590–8596.
[5] a) B. Piniello, E. Lira-Navarrete, H. Takeuchi, M. Takeuchi, R. S. Haltiwanger, R. Hurtado-Guerrero and C. Rovira, *ACS Catal.* **2021**, *11*, 9926–9932; b) B. Piniello, J. Macias-Leon, S. Miyazaki, A. Garcia-Garcia, I. Companon, M. Ghirardello, V. Taleb, B. Veloz, F. Corzana, A. Miyagawa, C. Rovira and R. Hurtado-Guerrero, *Nat. Commun.* **2023**, *14*, 5785; c) M. Kumari, S. Kozmon, P. Kulhánek, J. Štepán, I. Tvaroška and J. Koča, *J. Phys. Chem. B* **2015**, *119*, 4371–4381.
[6] A. Ardèvol and C. Rovira, *J. Am. Chem. Soc.* **2015**, *137*, 7528–7547.
[7] a) S. S. Lee, S. Y. Hong, J. C. Errey, A. Izumi, G. J. Davies and B. G. Davis, *Nat. Chem. Biol.* **2011**, *7*, 631–638; b) A. Ardèvol and C. Rovira, *Angew. Chem. Int. Ed. Engl.* **2011**, *50*, 10897–10901.
[8] a) H. Gomez, I. Polyak, W. Thiel, J. M. Lluch and L. Masgrau, *J. Am. Chem. Soc.* **2012**, *134*, 4743–4752; b) D. Albesa-Jove, F. Mendoza, A. Rodrigo-Unzueta, F. Gomollon-Bel, J. O. Cifuente, S. Urresti, N. Comino, H. Gomez, J. Romero-Garcia, J. M. Lluch, E. Sancho-Vaello, X. Biarnes, A. Planas, P. Merino, L. Masgrau and M. E. Guerin, *Angew. Chem. Int. Ed. Engl.* **2015**, *54*, 9898–9902; c) F. Mendoza, J. M. Lluch and L. Masgrau, *Org. Biomol. Chem.* **2017**, *15*, 9095–9107; d) E. Lira-Navarrete, J. Iglesias-Fernández, W. F. Zandberg, I. Companon, Y. Kong, F. Corzana, B. M. Pinto, H. Clausen, J. M. Peregrina, D. J. Vocadlo, C. Rovira and R. Hurtado-Guerrero, *Angew. Chem. Int. Ed. Engl.* **2014**, *53*, 8206–8210; e) M. K. Bilyard, H. J. Bailey, L. Raich, M. A. Gafitescu, T. Machida, J. Iglesias-Fernandez, S. S. Lee, C. D. Spicer, C. Rovira, W. W. Yue and B. G. Davis, *Nature* **2018**, *563*, 235–240; f) P. Ferreira, P. A. Fernandes and M. J. Ramos, *Chem. Eur. J.* **2021**, *27*, 13998–14006; g) I. Tvaroska, *Carbohydr. Res.* **2015**, *403*, 38–47.
[9] a) A. Monegal and A. Planas, *J. Am. Chem. Soc.* **2006**, *128*, 16030–16031; b) R. J. Blackler, S. M. L. Gagnon, R. Polakowski, N. L. Rose, R. B. Zheng, J. A. Letts, A. R. Johal, B. Schuman, S. N. Borisova, M. M. Palcic and S. V. Evans, *Glycobiology* **2016**, *27*, 370–380.
[10] N. Soya, Y. Fang, M. M. Palcic and J. S. Klassen, *Glycobiology* **2011**, *21*, 547–552.
[11] a) H. Gomez, J. M. Lluch and L. Masgrau, *J. Am. Chem. Soc.* **2013**, *135*, 7053–7063; b) A. Bobovska, I. Tvaroska and J. Kona, *Glycobiology* **2015**, *25*, 3–7.
[12] V. Rojas-Cervellera, A. Ardèvol, M. Boero, A. Planas and C. Rovira, *Chemistry* **2013**, *19*, 14018–14023.
[13] T. J. B. Forrester, O. G. Ovchinnikova, Z. Li, E. N. Kitova, J. T. Nothof, A. Koizumi, J. S. Klassen, T. L. Lowary, C. Whitfield and M. S. Kimber, *Nat. Commun.* **2022**, *13*, 6277.
[14] O. G. Ovchinnikova, E. Mallette, A. Koizumi, T. L. Lowary, M. S. Kimber and C. Whitfield, *Proc. Natl. Acad. Sci. USA* **2016**, *113*, E3120–3129.
[15] L. Doyle, O. G. Ovchinnikova, B.-S. Huang, T. J. B. Forrester, T. L. Lowary, M. S. Kimber and C. Whitfield, *J. Biol. Chem.* **2023**, *104609*.
[16] a) R. Anandakrishnan, B. Aguilar and A. V. Onufriev, *Nucleic Acids Res.* **2012**, *40*, W537–W541; b) T. P. Silverstein, *Prot. Sci.* **2021**, *30*, 735–744; c) J. C. Gordon, J. B. Myers, T. Folta, V. Shoja, L. S. Heath and A. Onufriev, *Nucleic Acids Res.* **2005**, *33*, W368–W371.
[17] M. J. Abraham, T. Murtola, R. Schulz, S. Páll, J. C. Smith, B. Hess and E. Lindahl, *SoftwareX* **2015**, *1*, 19–25.

[18] J. A. Maier, C. Martinez, K. Kasavajhala, L. Wickstrom, K. E. Hauser and C. Simmerling, *J. Chem. Theory Comput.* **2015**, *11*, 3696–3713.
[19] K. N. Kirschner, A. B. Yongye, S. M. Tschampel, J. Gonzalez-Outeirino, C. R. Daniels, B. L. Foley and R. J. Woods, *J. Comput. Chem.* **2008**, *29*, 622–655.
[20] W. L. Jorgensen, J. Chandrasekhar, J. D. Madura, R. W. Impey and M. L. Klein, *J. Chem. Phys.* **1983**, *79*, 926–935.
[21] D. A. Case, H. M. Aktulga, K. Belfon, D. S. Cerutti, G. A. Cisneros, V. W. D. Cruzeiro, N. Forouzesh, T. J. Giese, A. W. Götz, H. Gohlke, S. Izadi, K. Kasavajhala, M. C. Kaymak, E. King, T. Kurtzman, T.-S. Lee, P. Li, J. Liu, T. Luchko, R. Luo, M. Manathunga, M. R. Machado, H. M. Nguyen, K. A. O'Hearn, A. V. Onufriev, F. Pan, S. Pantano, R. Qi, A. Rahnamoun, A. Risheh, S. Schott-Verdugo, A. Shajan, J. Swails, J. Wang, H. Wei, X. Wu, Y. Wu, S. Zhang, S. Zhao, Q. Zhu, T. E. Cheatham, III, D. R. Roe, A. Roitberg, C. Simmerling, D. M. York, M. C. Nagan and K. M. Merz, Jr., *J. Chem. Inf. Model.* **2023**, *63*, 6183–6191.
[22] a) A. Bernardi, R. Faller, D. Reith, K. N. Kirschner, *SoftwareX* **2019**, *10*, 100241; b) A. W. Sousa da Silva, W. F. Vranken, *BMC Res. Notes* **2012**, *5*, 367.
[23] G. Bussi, D. Donadio, M. Parrinello, *J. Chem. Phys.* **2007**, *126*, 014101.
[24] M. Parrinello, A. Rahman, *J. Appl. Phys.* **1981**, *52*, 7182–7190.
[25] D. A. Case, H. M. Aktulga, K. Belfon, I. Y. Ben-Shalom, J. T. Berryman, S. R. Brozell, D. S. Cerutti, T. E. C. III, G. A. Cisneros, V. W. D. Cruzeiro, T. A. Darden, N. Forouzesh, M. Ghazimirsaeed, G. Giambaşu, T. Giese, M. K. Gilson, H. Gohlke, A. W. Goetz, J. Harris, Z. Huang, S. Izadi, S. A. Izmailov, K. Kasavajhala, M. C. Kaymak, A. Kovalenko, T. Kurtzman, T. S. Lee, P. Li, C. Lin, J. Liu, T. Luchko, R. Luo, M. Machado, M. Manathunga, K. M. Merz, Y. Miao, O. Mikhailovskii, G. Monard, H. Nguyen, K. A. O'Hearn, A. Onufriev, F. Pan, S. Pantano, A. Rahnamou, D. R. Roe, A. Roitberg, C. Sagui, S. Schott-Verdugo, A. Shajan, J. Shen, C. L. Simmerling, N. R. Skrynnikov, J. Smith, J. Swails, R. C. Walker, J. Wang, J. Wang, X. Wu, Y. Wu, Y. Xiong, Y. Xue, D. M. York, C. Zhao, Q. Zhu, P. A. Kollman in *Amber 2024. University of California, San Francisco.*, *Vol.* **2024**.
[26] T. D. Kuhne, M. Iannuzzi, M. Del Ben, V. V. Rybkin, P. Seewald, F. Stein, T. Laino, R. Z. Khaliullin, O. Schutt, F. Schiffmann, D. Golze, J. Wilhelm, S. Chulkov, M. H. Bani-Hashemian, V. Weber, U. Borstnik, M. Taillefumier, A. S. Jakobovits, A. Lazzaro, H. Pabst, T. Muller, R. Schade, M. Guidon, S. Andermatt, N. Holmberg, G. K. Schenter, A. Hehn, A. Bussy, F. Belleflamme, G. Tabacchi, A. Gloss, M. Lass, I. Bethune, C. J. Mundy, C. Plessl, M. Watkins, J. VandeVondele, M. Krack and J. Hutter, *J. Chem. Phys.* **2020**, *152*, 194103.
[27] J. Wang, R. M. Wolf, J. W. Caldwell, P. A. Kollman and D. A. Case, *J. Comput. Chem.* **2004**, *25*, 1157–1174.
[28] J. P. Perdew, K. Burke and M. Ernzerhof, *Phys. Rev. Lett.* **1996**, *77*, 3865–3868.
[29] S. Goedecker, M. Teter and J. Hutter, *Phys. Rev. B* **1996**, *54*, 1703–1710.
[30] J. VandeVondele and J. Hutter, *J. Chem. Phys.* **2007**, *127*, 114105.
[31] a) A. Laio and M. Parrinello, *Proc. Natl. Acad. Sci. USA* **2002**, *99*, 12562–12566; b) A. Barducci, M. Bonomi and M. Parrinello, *WIREs Comput. Mol. Sci.* **2011**, *1*, 826–843.
[32] G. A. Tribello, M. Bonomi, D. Branduardi, C. Camilloni and G. Bussi, *Comp. Phys. Commun.* **2014**, *185*, 604–613.
[33] D. W. Scott, *Biometrika* **1979**, *66*, 605–610.
[34] B. W. Silverman, *Density Estimation for Statistics and Data Analysis*, Springer US, **1986**, p.
[35] M. Sagiroglugil, Q. Liao, A. Planas, C. Rovira, *Dataset for* "Formation of a covalent adduct in retaining β-Kdo-glycosyltransferase WbbB via substrate-mediated proton relay", (1.0.0) [Data set] Zenodo **2024** https://zenodo.org/records/8385519.

Manuscript received: April 25, 2024
Revised manuscript received: June 7, 2024
Accepted manuscript online: July 22, 2024
Version of record online: September 12, 2024